TURBULENCE

Synthetic dissipation and cascade fluxes in a turbulent quantum gas

Nir Navon[1]*, Christoph Eigen[2], Jinyi Zhang[2], Raphael Lopes[2]†, Alexander L. Gaunt[2,3], Kazuya Fujimoto[4]*‡, Makoto Tsubota[5], Robert P. Smith[2,6], Zoran Hadzibabic[2]

Scale-invariant fluxes are the defining property of turbulent cascades, but their direct measurement is a challenging experimental problem. Here we perform such a measurement for a direct energy cascade in a turbulent quantum gas. Using a time-periodic force, we inject energy at a large length scale and generate a cascade in a uniformly trapped three-dimensional Bose gas. The adjustable trap depth provides a high-momentum cutoff k_D, which realizes a synthetic dissipation scale. This gives us direct access to the particle flux across a momentum shell of radius k_D, and the tunability of k_D allows for a clear demonstration of the zeroth law of turbulence. Moreover, our time-resolved measurements give unique access to the pre–steady-state dynamics, when the cascade front propagates in momentum space.

The discovery of a universal law describing the transfer of energy from large to small length scales in turbulent flows was a conceptual breakthrough (*1*, *2*). Despite their complex spatiotemporal dynamics, turbulent flows often obey a simple generic picture: The energy injected into the system at a large length scale is gradually transferred to ever smaller ones, flowing locally in Fourier space through the so-called inertial range where no dissipation occurs, until it is dissipated at some small length scale. In Fig. 1A, we depict such turbulent-cascade dynamics for a compressible field in real space. The field is initially at rest. At times $t > 0$, an external force creates excitations at a large length scale $1/k_F$. These excitations propagate to smaller length scales owing to their nonlinear interactions. Once they first reach the dissipation scale $1/k_D$, at time t_d, the field fluctuates on all length scales from $1/k_F$ to $1/k_D$. If a steady state is established within the momentum range k_F to k_D, from thereon energy is dissipated at k_D at the same rate at which it is injected at k_F. In such a steady state, the momentum-space distributions of quantities such as the energy or wave amplitude are generically scale-free power laws.

Many quantitative theoretical predictions about turbulence are based on taking the mathematical limits $k_F \to 0$ and $k_D \to \infty$ (*3*). Such formal treatments lead to predictions that are elegant but often counterintuitive. A key prediction of this kind is that for $k_D \to \infty$, the steady-state cascade corresponds to a scale-invariant (k-independent) energy flux through momentum space, but no particle flux (*4*).

Experimentally, the steady-state power-law spectra of various quantities have been extensively studied (*5*–*9*), whereas the equally fundamental cascade fluxes are harder to measure (*10*–*13*). Recently, ultracold atomic gases have emerged as a versatile platform for studies of turbulence (*9*, *14*–*22*), offering experimental possibilities unavailable in other systems. Here, we use an atomic gas to directly measure cascade fluxes in a turbulent system. Our dissipation scale is tuneable, which allows us to explore how the fluxes depend on k_D, and to reconcile the experimental observations with the formal predictions for $k_D \to \infty$. Our system also allows a time-resolved study of the initial stage of turbulence (*23*–*25*), when a steady state is not yet established, which reveals how the cascade front propagates in momentum space.

Our experiment starts with a weakly interacting Bose-Einstein condensate of $N \approx 1.2 \times 10^5$ atoms of ^{87}Rb in the uniform potential of a cylindrical optical box trap of radius $R \approx 16\ \mu$m and length $L \approx 27\ \mu$m (Fig. 1B) (*26*). At the end of the initial preparation of the gas, the noncondensed fraction is <10% and the chemical potential is $\mu \approx k_B \times 2$ nK, corresponding to a healing length $\xi \approx 1.2\ \mu\text{m} \ll R, L$. We initiate a turbulent cascade by injecting energy at the system-size length scale (corresponding to a small momentum k_F), using a spatially uniform force $\mathbf{F}_s(\mathbf{r}, t) = F_0 \sin(\omega_s t)\hat{\mathbf{x}}$, where $\hat{\mathbf{x}}$ is a unit vector along the box symmetry axis, $F_0 L \approx k_B \times 2.5$ nK, and $\omega_s \approx 2\pi \times 9$ Hz is tuned to resonantly excite the sound wave of wavelength $2L$ (so $k_F = \pi/L$) (*27*). This anisotropic forcing of the matter-wave field is represented in Fig. 1C as a small dark blue area elongated along k_x. As shown in (*9*), after several seconds of shaking, the momentum distribution of the gas in the inertial range is statistically isotropic and time-invariant, $n(\mathbf{k}, t) \approx \langle n(k) \rangle \propto k^{-\gamma}$, with $\gamma \approx 3.5$ (*28*, *29*). The time invariance implies that the energy and particle fluxes through this k-range are k-independent, but it does not reveal their values. Here, we extract the cascade fluxes by studying the dissipation in our gas.

In conventional fluids, one observes macroscopic (hydrodynamic) degrees of freedom, and the dissipation occurs in the form of heating (i.e., transfer of energy into the microscopic degrees of freedom). This dissipation is set by the viscosity ν, which is generally not tuneable. Moreover, the resulting minute heating is often difficult to measure because of thermal coupling of the fluid with its surroundings (*30*). Our system is thermally isolated from the environment, and we have direct access to all the microscopic degrees of freedom, so the dissipation occurs only in the form of (readily measurable) particle loss. The optical box (Fig. 1B) has a non-infinite energy depth U_D, so particles with a sufficiently large energy leave the box; in momentum space, U_D corresponds to a sphere of radius $k_D = \sqrt{2mU_D}/\hbar$ (Fig. 1C), where m is the atom mass and $\hbar$ is Planck's constant divided by 2π. This simple feature realizes a synthetic dissipation scale, with U_D defining the particle and energy sink. Crucially, this dissipation scale can be tuned by changing the trapping laser power (*31*).

Formally, within the assumptions of the wave-turbulence theory, the equations of motion lead to a continuity equation, with a source and a sink, that is local in momentum space (*3*):

$$\frac{\partial n(\mathbf{k}, t)}{\partial t} = F(\mathbf{k}, t) - D(\mathbf{k}, t) - \nabla_{\mathbf{k}} \cdot \mathbf{\Pi}_n(\mathbf{k}, t) \quad (1)$$

Here $F(\mathbf{k}, t)$ corresponds to the external force, $D(\mathbf{k}, t)$ describes the dissipation, and $\nabla_{\mathbf{k}} \cdot \mathbf{\Pi}_n$ captures the nonlinear interactions, where $\mathbf{\Pi}_n$ is the particle flux. For $F = D = 0$, the steady-state solutions are zero-flux equilibrium thermodynamic states. If F and D are nonzero but are localized in k space, one can also get nonequilibrium steady-state solutions with a nonzero scale-independent flux sustained by the source F and the sink D.

For an isotropic outflow, the total radial particle flux is $\Pi_n(k) = 4\pi k^2 |\mathbf{\Pi}_n(\mathbf{k})|$. Hence, from Eq. 1, in the inertial range $4\pi k^2\, \partial n/\partial t = -\partial \Pi_n/\partial k$. Integrating over k shows that we can measure the particle flux through the shell at k_D by simply counting the atoms remaining in the trap (see Fig. 1C):

$$\frac{\partial N}{\partial t} \equiv -\Pi_n(k_D, t) \quad (2)$$

[1]Department of Physics, Yale University, New Haven, CT 06520, USA. [2]Cavendish Laboratory, University of Cambridge, Cambridge CB3 0HE, UK. [3]Microsoft Research, Cambridge CB1 2FB, UK. [4]Department of Physics, University of Tokyo, 7-3-1 Hongo, Bunkyo-ku, Tokyo 113-0033, Japan. [5]Department of Physics and Nambu Yoichiro Institute of Theoretical and Experimental Physics, Osaka City University, 3-3-138 Sugimoto, Sumiyoshi-Ku, Osaka 558-8585, Japan. [6]Clarendon Laboratory, University of Oxford, Oxford OX1 3PU, UK.
*Corresponding author. Email: nir.navon@yale.edu (N.N.); kazuya_fujimoto@rover.nuap.nagoya-u.ac.jp (K.F.) †Present address: Laboratoire Kastler Brossel, Collège de France, CNRS, ENS-PSL University, UPMC-Sorbonne Université, F-75005 Paris, France. ‡Present address: Institute for Advanced Research, Nagoya University, Nagoya 464-8601, Japan.

For a (non-equilibrium) steady state, with time-invariant $n(k)$ in the inertial range (*9*), the particle flux is k- and t-independent (*32*), so $\Pi_n(k_D, t) = \Pi_n(k, t) = \Pi_n$.

In steady state, the total radial energy flux, $\Pi_\mathcal{E}(k, t)$, is also k- and t-independent in the inertial range, and is equal to the rate of energy dissipation. To relate it to Π_n, we consider the pertinent case of weakly interacting particles with a dispersion relation $\omega(k)$, so the energy spectrum is $\mathcal{E}(k, t) = \hbar\omega(k)n(k, t)$; in our case, $\omega(k) \propto k^2$. At $k < k_D$, microscopic interactions drive particles to both lower and higher k, so the relationship between the net energy and particle fluxes, $\Pi_\mathcal{E}$ and Π_n, is nontrivial; one might naïvely expect that $\Pi_\mathcal{E}(k) = \hbar\omega(k)\Pi_n(k)$, but this cannot be true if both $\Pi_\mathcal{E}$ and Π_n are k-independent and $\omega(k)$ is not. However, at k_D the particles flow only one way because there is no "backflow" from the sink into the inertial range, so one can intuitively write

$$\Pi_\mathcal{E}(k_D) = \hbar\omega(k_D)\ \Pi_n(k_D) \qquad (3)$$

Steady state then requires $\Pi_\mathcal{E} = \hbar\omega(k_D)\Pi_n$ at all k in the inertial range; for our $\omega(k)$, this means that $\Pi_\mathcal{E} \propto {k_D}^2\Pi_n$. To formally derive Eq. 3, one multiplies Eq. 1 by $\hbar\omega(k)$ and invokes the continuity equation for the energy to obtain

$$\frac{\partial\Pi_\mathcal{E}(k,t)}{\partial k} = \hbar\omega(k)\frac{\partial\Pi_n(k,t)}{\partial k} \qquad (4)$$

in the inertial range. For $k < k_D$, this equation is trivially satisfied by both of its sides being zero, and does not impose any relation between $\Pi_\mathcal{E}(k)$ and $\Pi_n(k)$. However, integrating it across a shell around k_D, and setting $n(k)$ and all fluxes to zero for $k > k_D$, recovers Eq. 3.

Experimentally, we vary k_D while keeping F_0 fixed and measure $\Pi_n(k_D)$ according to Eq. 2. To mitigate the effects of the long-term few-percent drifts in the initial N, and of the additional atom loss through collisions with the background-gas particles, we perform differential measurements of the cascade-induced atom loss, N_{loss}, with reference measurements taken by setting F_0 to zero in an otherwise identical experimental sequence.

In Fig. 2, we show N_{loss} as a function of the shaking time t_s for various values of U_D. In all cases at short times, we observe no loss (within error). This is consistent with the expectations that no losses occur at $k < k_D \propto \sqrt{U_D}$ and that initially it takes time for the excitations to cascade to k_D, when a steady state can be established (see Fig. 1). For t_s longer than some onset time t_d, the loss rate $\partial N_{loss}/\partial t$ is essentially constant in time, as long as the total loss is relatively small (<30% of the initial $N \approx 1.2 \times 10^5$). The dashed lines show piecewise linear fits that we use to extract, for each U_D, both t_d and the subsequent initial loss rate, which we identify with the steady-state particle flux $\Pi_n = \Pi_n(k_D)$. At much longer times, $t_s \gg t_d$, the steady-state assumption can no longer hold, because the losses gradually deplete the low-k source of atoms.

In Fig. 3, we show a log-log plot of Π_n versus U_D (*31*). We observe power-law behavior with $\Pi_n \propto {U_D}^{-1.05\pm0.08} \propto {k_D}^{-2.10\pm0.16}$. We complement these measurements with numerical simulations based on the Gross-Pitaevskii equation, for the same forcing protocol and without any free parameters [see (*27*) for details]. The numerical simulation results are shown by solid circles; a fit to the numerical data gives $\Pi_n \propto {U_D}^{-1.04\pm0.01}$, in good agreement with the experimental data.

The so-called zeroth law of turbulence, first formulated in the context of classical incompressible fluids, stipulates that for fixed forcing, the steady-state rate of energy dissipation tends to a nonzero constant as the viscosity vanishes ($\nu \to 0$) (*5*, *33*). In our case, this corresponds to keeping F_0 fixed and taking $k_D \to \infty$ (*34*). This

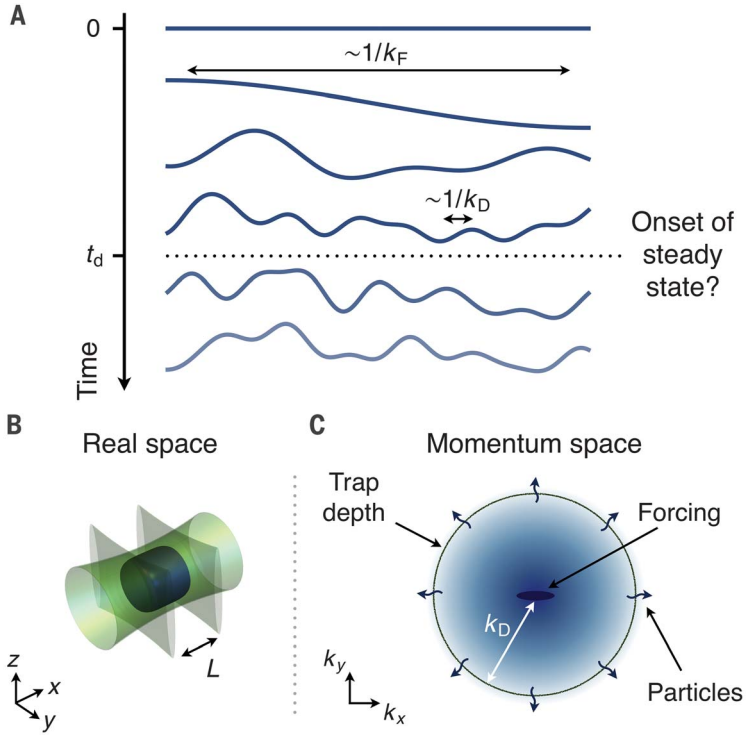

Fig. 1. Turbulent cascade in a box-trapped quantum gas. (**A**) Cartoon of real-space dynamics of a turbulent wave. Energy is injected by applying a force at a large length scale, $1/k_F$, and propagates to smaller scales because of nonlinear interactions. A steady state can be established when the excitations first reach the small dissipation length scale, $1/k_D$, at time t_d. (**B**) Sketch of the experimental setting. The atoms are trapped in a finite-depth potential in the shape of a cylindrical box, formed by laser barriers. The shaking force is applied along the x axis. (**C**) In momentum space, the dissipation scale k_D is set by the trap depth; when excitations propagate to k_D, dissipation occurs in the form of particle loss.

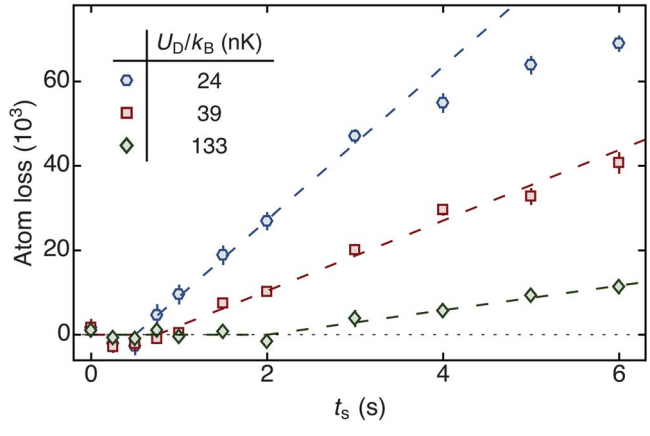

Fig. 2. Atom-loss dynamics associated with the turbulent cascade. The graph shows atoms lost versus shaking time t_s for different trap depths U_D (at $t_s = 0$, the atom number is $N \approx 1.2 \times 10^5$). Data points show averages of typically 50 measurements. Dashed lines are piecewise linear fits. The systematic uncertainty in U_D values is 20%.

law implies that the particle flux should vanish as $\Pi_n \sim k_D^{-2}$ (see Eq. 3), in excellent agreement with our data. Note that the steady-state energy balance also requires that $\Pi_\mathcal{E}$ is equal to the rate of energy input into the system, ε. However, energy conservation alone is not sufficient to predict the scaling of Π_n with k_D, because it is not a priori obvious that for fixed F_0 the rate at which the system absorbs energy from the drive is not affected by changing k_D (*35*). Only a posteriori, from Fig. 3 (and the conservation of energy), can we see that in our system the steady-state ε must be independent of the dissipation length scale down to our lowest k_D. If k_D were changed dynamically, for a system to reach a new steady state the particle flux would have to self-consistently adjust at all $k_F < k < k_D$, because the steady-state Π_n must be both k_D-dependent (to satisfy the zeroth law) and k-independent for a given k_D.

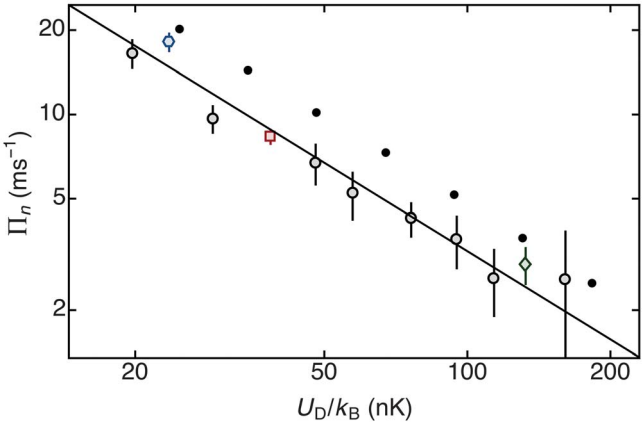

Fig. 3. Steady-state particle flux. The atom-loss rate Π_n versus the dissipation energy scale U_D (open symbols) is shown on a log-log plot; the three colored points correspond to the data shown in Fig. 2. Solid symbols show the results of numerical simulations (*27*). The systematic uncertainty in U_D values is 20%. A power-law fit to the experimental data (solid line) gives $\Pi_n \propto U_D^{-1.05\pm0.08} \propto k_D^{-2.10\pm0.16}$, in agreement with the theoretical prediction.

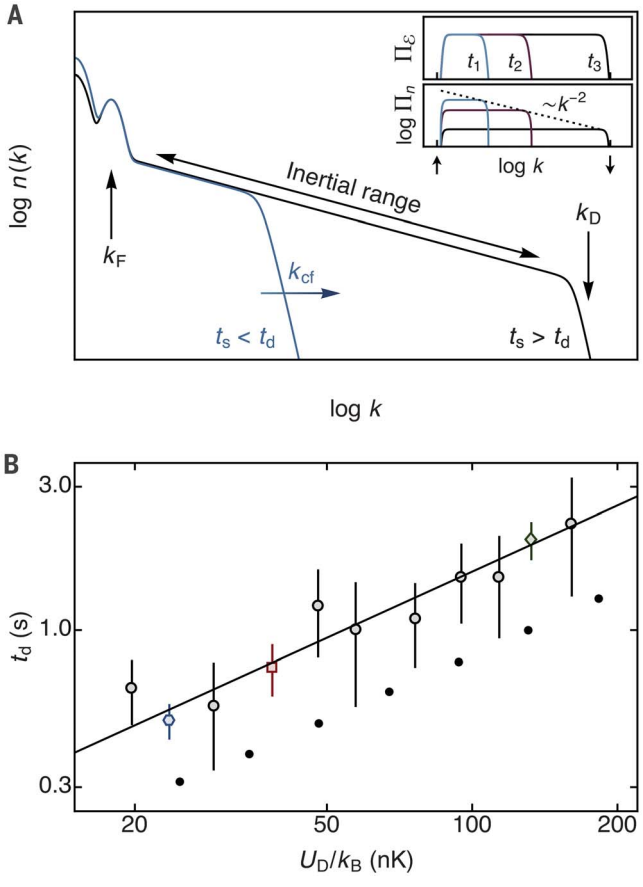

Fig. 4. Establishing the steady state: The cascade-front dynamics. (**A**) Momentum-space turbulent dynamics. Forcing occurs at k_F and the steady-state distribution $n(k)$ is established in the wake of the cascade front $k_{cf}(t_s)$, which propagates outward until it reaches k_D at time t_d. For clarity, here we show an idealized sketch with a very large separation between k_F and k_D; see (*27*) for numerical simulations with our experimental parameters. Inset: Consistent picture for the evolution of the energy flux $\Pi_\mathcal{E}$ and particle flux Π_n for three different times, t_1 (blue) < t_2 (purple) < t_3 (black), with $t_2 < t_d < t_3$. The forcing and dissipation scales are indicated by the vertical arrows, as in the main panel. (**B**) Onset time for dissipation. Open symbols show the measured t_d values versus U_D on a log-log plot; the three colored points correspond to the data shown in Fig. 2. Solid symbols show the results of numerical simulations (*27*). The systematic uncertainty in U_D values is 20%. A power-law fit, $t_d \propto U_D^\beta$, to the experimental data (solid line) gives $\beta = 0.73 \pm 0.06$, in agreement with the prediction $\beta = 0.75 \pm 0.05$.

Having established a consistent picture of the steady-state fluxes in our gas, we now turn to the pre–steady-state turbulent dynamics. In Fig. 4A, we depict the early-time dynamics in Fourier space. The forcing, which generates a surplus of atoms at k_F, initiates the cascade at $t_s = 0$. As the cascade front, $k_{cf}(t_s)$, propagates to higher k, the steady-state momentum distribution, $n(k) \propto k^{-\gamma}$, is established in its wake [see also (*27*)]. The dynamics are dissipationless until k_{cf} reaches k_D (at time t_d); only then is a steady state, with matching ε and $\Pi_\mathcal{E}(k_D)$, established. Hence, our experimental observations of the initial dissipationless stage of turbulence ($t_s < t_d$), and the dependence of t_d on U_D, give us access to the dynamics of the cascade front in momentum space.

At $t_s < t_d$, the instantaneous particle flux is k-independent for $k < k_{cf}(t_s)$, vanishes for $k > k_{cf}(t_s)$, and must match the rate of the population increase in the inertial range: $n(k_{cf})4\pi k_{cf}^2 dk_{cf} = \Pi_n(k_{cf})dt_s$, so $k_{cf}^{2-\gamma}dk_{cf} \propto \Pi_n(k_{cf})dt_s$. Analogously, for the increase of total energy in the inertial range, $k_{cf}^{4-\gamma}dk_{cf} \propto \Pi_\mathcal{E}(k_{cf})dt_s$, and $\Pi_\mathcal{E}(k_{cf})$ is equal to the instantaneous energy injection rate ε.

Assuming that ε, which we found not to depend on k_D in steady state, is also independent of k_{cf} at $t_s < t_d$, then the instantaneous $\Pi_n(t_s)$, at $k < k_{cf}(t_s)$, is $\propto k_{cf}^{-2}$. This gives an elegant unifying picture of the particle fluxes for $t_s < t_d$ and $t_s > t_d$ [Fig. 4A, inset, and (*27*)]: Π_n is always the same function of the highest k for which the steady-state $n(k)$ has been established (i.e., the lowest k from which there is no backflow), whether that is the instantaneous $k_{cf} < k_D$ (for $t_s < t_d$) or k_D. This self-consistent picture also leads to a quantitative prediction that is verifiable in our experiments: The time independence of ε implies $k_{cf}^{4-\gamma}dk_{cf} \propto dt_s$, which for $\gamma < 5$ and $k_D \gg k_F$ gives a power-law prediction $t_d \propto U_D^\beta$, with $\beta = (5 - \gamma)/2$. Specifically, for our $\gamma = 3.5 \pm 0.1$ (*9*), we predict $\beta = 0.75 \pm 0.05$.

In Fig. 4B, we show the variation of t_d with U_D. We find that our data are indeed well described by a power law, with $\beta = 0.73 \pm 0.06$, in agreement with our prediction. The results of our numerical simulations (solid circles) show similar behavior with a small systematic offset; a fit to the numerical data gives $\beta = 0.71 \pm 0.01$.

Finally, we note that the criterion for t_d to show scaling behavior, namely $\gamma < 5$ and hence $\beta > 0$, is intimately linked to another important concept in the theory of turbulence. For $\gamma < 5$, the steady-state spectrum has infinite

energy capacity, meaning that it carries infinite energy for $k_D \to \infty$. It is indeed generally expected for infinite-capacity systems that the cascade front propagates at a finite speed and that the Kolmogorov-Zakharov turbulence spectrum forms behind it (*36*).

Our work provides a complete, consistent picture of the wave turbulence dynamics at both short (pre–steady-state) and long (steady-state) times. In the broader context of far-from-equilibrium many-body quantum systems, a turbulent quantum gas with a large k_D provides a particularly interesting example of an essentially stationary nonthermal state [see also (*37*–*39*)]. The possibility of synthetic dissipation also opens new theoretical perspectives. In the future it would be interesting to engineer arbitrary momentum-cutoff landscapes, which could, for example, allow studies of anisotropic turbulence. By dynamically tuning the dissipation scale or the driving force, it should also be possible to study quenches between different turbulent states.

REFERENCES AND NOTES

1. A. N. Kolmogorov, *Dokl. Akad. Nauk SSSR* **30**, 299–303 (1941).
2. A. Obukhov, *Dokl. Akad. Nauk SSSR* **32**, 22–24 (1941).
3. V. E. Zakharov, V. S. L'vov, G. Falkovich, *Kolmogorov Spectra of Turbulence* (Springer, 1992).
4. S. Dyachenko, A. Newell, A. Pushkarev, V. Zakharov, *Physica D* **57**, 96–160 (1992).
5. U. Frisch, *Turbulence: The Legacy of A. N. Kolmogorov* (Cambridge Univ. Press, 1995).
6. O. Alexandrova *et al*., *Phys. Rev. Lett.* **103**, 165003 (2009).
7. J. Salort *et al*., *Phys. Fluids* **22**, 125102 (2010).
8. A. Chepurnov, B. Burkhart, A. Lazarian, S. Stanimirovic, *Astron. J.* **810**, 33 (2015).
9. N. Navon, A. L. Gaunt, R. P. Smith, Z. Hadzibabic, *Nature* **539**, 72–75 (2016).
10. W. D. McComb, *Homogeneous, Isotropic Turbulence: Phenomenology, Renormalization and Statistical Closures* (Oxford Univ. Press, 2014).
11. M. S. Uberoi, *Phys. Fluids* **6**, 1048 (1963).
12. M. Miyake, M. Donelan, Y. Mitsuta, *J. Geophys. Res.* **75**, 4506–4518 (1970).
13. L. Deike, M. Berhanu, E. Falcon, *Phys. Rev. E* **89**, 023003 (2014).
14. E. A. L. Henn, J. A. Seman, G. Roati, K. M. F. Magalhães, V. S. Bagnato, *Phys. Rev. Lett.* **103**, 045301 (2009).
15. T. W. Neely *et al*., *Phys. Rev. Lett.* **111**, 235301 (2013).
16. W. J. Kwon, G. Moon, J. Choi, S. W. Seo, Y. Shin, *Phys. Rev. A* **90**, 063627 (2014).
17. M. C. Tsatsos *et al*., *Phys. Rep.* **622**, 1–52 (2016).
18. W. J. Kwon, J. H. Kim, S. W. Seo, Y. Shin, *Phys. Rev. Lett.* **117**, 245301 (2016).
19. S. W. Seo, B. Ko, J. H. Kim, Y. Shin, *Sci. Rep.* **7**, 4587 (2017).
20. M. E. Mossman, M. A. Hoefer, K. Julien, P. G. Kevrekidis, P. Engels, *Nat. Commun.* **9**, 4665 (2018).
21. S. P. Johnstone *et al*., *Science* **364**, 1267–1271 (2019).
22. G. Gauthier *et al*., *Science* **364**, 1264–1267 (2019).
23. B. V. Svistunov, *J. Mosc. Phys. Soc.* **1**, 373 (1991).
24. D. V. Semikoz, I. I. Tkachev II, *Phys. Rev. Lett.* **74**, 3093–3097 (1995).
25. D. V. Semikoz, I. I. Tkachev, *Phys. Rev. D Part. Fields* **55**, 489–502 (1997).
26. A. L. Gaunt, T. F. Schmidutz, I. Gotlibovych, R. P. Smith, Z. Hadzibabic, *Phys. Rev. Lett.* **110**, 200406 (2013).
27. See supplementary materials.
28. The exponent $\gamma \approx 3.5$ is close to the Kolmogorov-Zakharov prediction for (compressible) weak-wave turbulence in three dimensions, $\gamma = 3$, and in agreement with numerical simulations of the Gross-Pitaevskii equation (*9*), as well as with a scaling analysis of kinetic equations (*29*).
29. I. Chantesana, A. P. Orioli, T. Gasenzer, *Phys. Rev. A* **99**, 043620 (2019).
30. O. Cadot, Y. Couder, A. Daerr, S. Douady, A. Tsinober, *Phys. Rev. E* **56**, 427–433 (1997).
31. The lowest U_D we explore corresponds to $U_D/\mu \approx 10$, $U_D/(F_0 L) \approx 8$, and $k_D/k_F \approx 23$.
32. Note that it is the total radial flux Π_n, rather than $|\mathbf{\Pi}_n|$, that is k-independent in the inertial range.
33. J. C. Vassilicos, *Annu. Rev. Fluid Mech.* **47**, 95–114 (2015).
34. For incompressible flows, the Kolmogorov dissipation length scale, analogous to our $1/k_D$, depends on the viscosity of the fluid (as $\propto \nu^{3/4}$).
35. In most familiar systems, such as the damped harmonic oscillator, the rate at which the system absorbs energy in steady state depends on both the driving and the dissipation.
36. S. Nazarenko, *Wave Turbulence* (Springer, 2011).
37. M. Prüfer *et al*., *Nature* **563**, 217–220 (2018).
38. C. Eigen *et al*., *Nature* **563**, 221–224 (2018).
39. S. Erne, R. Bücker, T. Gasenzer, J. Berges, J. Schmiedmayer, *Nature* **563**, 225–229 (2018).
40. N. Navon *et al*., Research data and code supporting "Synthetic dissipation and cascade fluxes in a turbulent quantum gas". Apollo (2019).

ACKNOWLEDGMENTS

We thank E. Altman, D. Stamper-Kurn, F. Chevy, and J. Glidden for discussions; T. Hilker for comments on the manuscript; and M. Matsumoto and T. Nishimura for a routine used in the numerical simulations. **Funding:** Supported by EPSRC grants EP/N011759/1 and EP/P009565/1, ERC (QBox), QuantERA (NAQUAS, EPSRC grant EP/R043396/1), AFOSR, and ARO; Trinity College, Cambridge (N.N. and A.L.G.); the David and Lucile Packard Foundation (N.N.); E.U. Marie-Curie program grant MSCA-IF-2015 704832 and Churchill College, Cambridge (R.L.); the Royal Society (R.P.S.); JSPS KAKENHI grant JP16J01683 (K.F.); and JSPS KAKENHI grant 17K05548 and MEXT KAKENHI grant 16H00807 (M.T.). **Author contributions:** N.N. initiated the project. N.N., C.E., and J.Z. collected the data. N.N. and C.E. analyzed the data. K.F. and M.T. performed the numerical simulations. Z.H. supervised the project. All authors contributed extensively to the interpretation of the data and the writing of the manuscript. **Competing interests:** The authors declare no competing interests. **Data and materials availability:** The data that support the findings of this study and the relevant numerical code are available in the Apollo repository (*40*).

SUPPLEMENTARY MATERIALS

science.sciencemag.org/content/366/6463/382/suppl/DC1
Supplementary Text
Figs. S1 to S3
References (*41*–*44*)

28 June 2019; accepted 24 September 2019
Published online 3 October 2019
10.1126/science.aau6103

Science

Synthetic dissipation and cascade fluxes in a turbulent quantum gas

Nir NavonChristoph EigenJinyi ZhangRaphael LopesAlexander L. GauntKazuya FujimotoMakoto TsubotaRobert P. SmithZoran Hadzibabic

Science, 366 (6463), • DOI: 10.1126/science.aau6103

Down and down the energy cascade

Injecting energy into a turbulent system at large length scales results in the energy cascading down and eventually dissipating at a characteristic small length scale. In conventional fluids, this small scale is set by fluid viscosity. Navon *et al.* studied the turbulence energy cascade in a quantum gas, a Bose-Einstein condensate of rubidium-87 atoms held in a uniform trap. Dissipation occurred by atoms escaping from the trap at a scale that could be tuned by varying the height of the trapping potential. Thanks to the flexibility of their setup, the researchers were able to study both the steady state, in which energy is injected at the same rate it is dissipated, and the transient regime preceding the steady state.

Science, this issue p. 382

Science (ISSN 1095-9203) is published by the American Association for the Advancement of Science. 1200 New York Avenue NW, Washington, DC 20005. The title *Science* is a registered trademark of AAAS.